Assessment of floating and yaw stability of a self-aligning floating offshore wind turbine

Stefan Netzband, Christian W. Schulz, Moustafa Abdel-Maksoud

Institute for Fluid Dynamics and Ship Theory, Hamburg University of Technology, Am Schwarzenberg-Campus 4, 21073 Hamburg, Germany

stefan.netzband@tu-harburg.de, christian.schulz@tu-harburg.de, m.abdel-maksoud@tu-harburg.de

Stefan Netzband: 2012 Dipl.-Ing., Hamburg University of Technology, 2012 Development engineer at TEMBRA GmbH & Co. KG, 2014 Research Assistant, Hamburg University of Technology. Main research fields: Simulation of the motion behaviour of floating offshore wind turbines.

Christian Schulz: 2016 M.Sc., Hamburg University of Technology, 2016 Research Assistant, Hamburg University of Technology. Main research fields: Aerodynamic simulation of (floating) wind turbines.

Moustafa Abdel-Maksoud: 1992, Dr.-Ing., Institute of Ship and Ocean Technology, Technical University of Berlin, 1995 Head of Numerical Simulation Department, at Potsdam Model Basin, 2003 Professor of Ship Technology at the Institute of Ship Technology and Transport systems, Duisburg-Essen University, 2007 Professor of Ship Theory, Hamburg University of Technology. Main research fields: Numerical Simulation of Flow Behaviour on Ship Hulls and Propulsion Systems, Renewable Maritime Energy.

Assessment of floating and yaw stability of a self-aligning floating offshore wind turbine

Floating Offshore Wind Turbines (FOWTs) are a promising concept to increase the expansion of offshore wind energy. In comparison with fix founded Offshore Wind Turbines (OWT), the overall cost is less dependent on the water depth, which leads to a variety of potential locations and markets worldwide. Furthermore, floating platforms allow for new structural designs with the potential to save material and installation cost. In this paper, a self-aligning platform equipped with a 6 MW Turbine is presented. The platform is moored on a single point and uses a turret buoy to be able to rotate freely around its anchor point. A downwind rotor and an airfoil-shaped tower induce self-aligning turning moments to follow changes of the wind direction passively. The first order boundary element method panMARE is used to simulate the motion behaviour considering aerodynamic, hydrodynamic and mooring loads. The self-aligning capability is demonstrated under partial turbine load for steady and dynamic conditions with waves and current.

Keywords: Panel Method; Boundary Element Method, Self-Aligning Floating Offshore Wind Turbine

Introduction

During the past decades, the wind turbine industry made the step from onshore to offshore with bottom fixed support structures like gravity foundations, jackets and monopiles. But with increasing water depth, the foundations becoming and more costly. An obvious next step is therefore the development of floating platforms. Based on the designs of oil and gas platforms (spar buoy, semisubmersible and tension leg platform) various types of floating offshore wind turbines (FOWT) have been developed world wide. Most of them adapt conventional turbine designs from fix foundations to floating platforms with the attempt to reduce the platform motion to a minimum. Some designs

include new turbine concepts and try to use the advantages of the floating platform.

In this paper, the SelfAligner of Cruse Offshore GmbH, see Figure fig:LOFT, is analysed. The floater is based on the principles of a semisubmersible platform. Key point of the concept is a single point mooring (SPM) which allows rotations of the platform around the vertical axis. The SCD 6MW downwind rotor of aerodyn engineering gmbh and a profiled tower induce pivoting moments to align the entire platform with the wind, see Figure fig:selfaligning (a). A yaw bearing and yaw controller is not required. But the main part of the turbine can be adapted from conventional down wind turbines. Since the tower has a fixed connection to the turbine housing, the structural design can be optimized for one-sided loads and its profile shape reduces tower shadow effects on the blade loads, see Figure fig:selfaligning (b).

Predicting the motion behaviour is a crucial issue in the development and design of the platform and tower structure. The interaction of aerodynamic loads on the rotor and the tower, hydrodynamic loads on the platform and mooring line forces must be calculated in an integrated simulation method. It is important to estimate the aerodynamic forces even for higher misalignment and predict the hydrodynamic pressure for large displacements with waves and in the presence of currents. The simulation of the mooring system is required to include all significant forces for the motion prediction and alignability.

The number of numerical simulation methods of flow induced loads and dynamic behaviour of FOWT has been growing in the past years. Most of them have their origin in the calculation of loads on onshore wind turbines. They have been extended to the application on OWT and are now even include hydrodynamic tools to simulate the motion of floating platforms. The turbine simulation is usually based on the blade element momentum theory (BEMT). A semi-empirical approach in which a rotor

blade is cut into several two-dimensional sections. Based on the momentum theory and lift and drag coefficients the forces on each element are calculated and then integrated over the entire rotor. Correction factors are applied to include three dimensional effects and losses. But since the flow field is not modelled, interactions between the rotor and transient changes in the wake are not considered. A good agreement of simulation results and experimental values are shown among others by Laino et al. (2002) for a turbine which is aligned as well as slightly deviated from the main wind direction.

Most of the hydrodynamic tools for the estimation of platform forces use frequency-domain based formulations and/or Morison equation (Cordle and Jonkman 2011). For the first, frequency-dependent coefficient matrices are calculated in a preceding step using three dimensional panel methods. They describe the global motion characteristic and include hydrostatic, radiation, diffraction and added mass effects. However, frequency-domain based formulations are only valid for periodic motions and coupled systems exceed the limits of the theory. The viscous effects like platform drag cannot be covered. The impulse response function method can be applied to calculate the hydrodynamic forces in time-domain. In this case the wave induced forces and the damping will be based on the frequency-domain results. The hydrodynamic solution of the problem can be simplified by assuming the dimension of the structure are small and do not have a considerable influence on the incoming waves. In this case the Morison equation can be applied, which is a semi-empirical approach based on added-mass and drag coefficients. The Morison equation is evaluated on every single part of the platform and especially for cylindrical structures. But the flow field is not modelled and therefore no fluid interaction is considered.

The mooring system is usually simulated using either a quasi-static approach or dynamic method. Quasi-static approaches account for the forces of a hanging line with

constant diameter and weight (Masciola 2015). Additional fluid forces or inertia are neglected. Dynamic methods are based on lumped-mass models (Hall and Goupee 2015) or even finite element analysis and can include fluid forces, inertia and platform motions. Especially in unsteady cases with large motions such as extreme load cases, large differences between quasi-static and dynamic mooring models have been shown by Hall (2014).

For a time-domain simulation, aerodynamic, hydrodynamic and mooring forces are combined in a six-degrees-of-freedom solver (6DOF) to estimate the motions. An implicit integration scheme is usually used to achieve convergence between the motion state and all three domains.

However, for the simulation of a self-aligning FOWT, large rotor yaw angles needs to be simulated and the lift force of the tower as well as drag forces on the platform are important to consider. Since BEMT is a two-dimensional approach, the ability to simulate three-dimensional effects, and hereby non-axial flow on a horizontal axis turbine or large rotor cone angles, is limited.

A new approach based on the boundary element method (BEM) *pan*MARE has been presented previously (Netzband et al. 2018). In both domains, aerodynamic and hydrodynamic, the geometries are discretized using first-order panels and the inviscid flow fields are solved for the current motion state. The direct representation of the platform with its instantaneous position and wave elevation allows for a detailed calculation of the wetted hull surface area. Additional elements are used to include the hull drag induced by viscous flow effects which are not covered by potential flow. Solving the aerodynamic flow field allows for the simulation of the wake interaction with the rotor blades and resolve effects induced by the platform motion and non-axial flow. While using the same code for both fluid domains, a strong coupling is realized

which allows for an explicit time-integration using a higher-order integration scheme. A comparison of the results with a selection of the Offshore Code Comparison Collaboration Continuation (OC4) (Robertson et al. 2014) shows good agreement for a couple of load cases.

In the following, the model of the self-aligning FOWT in *pan*MARE is described. Additional elements are introduced to include the forces of the tower and direction depending drag. Moreover a dynamic mooring model is implemented which is described shortly. Basic dimensions of the platform, tower and rotor are given in a separate section. Following on the setup description, results of the simulations are presented. First the floating and self-aligning capability for partial load with and without oblique current gives a valuation for steady conditions. Afterwards the dynamic behaviour with increasing wind speed and direction change at the same time is shown.

Method

The three-dimensional first-order panel method panMARE was at first developed for the simulation of ship propellers (Bauer and Abdel-Maksoud 2012, Hundemer 2013). In the following time it has been extended for the simulation of floating structures in time domain (Schoop-Zipfel and Abdel-Maksoud 2014). The ability of rotor flow and floating body simulation has been merged for the simulation of FOWT in the nearer past (Netzband et al. 2018). The underlying theory and most important parts of the simulation method for the self-aligning FOWT are presented in this section. Most of the model details are similar to the previous paper and therefore are briefly described. In addition, some further improvements have been implemented, which are provided below.

The general coordinate system is shown in Figure fig:COS. It is located at the still water line (SWL) in the centre of the anchors. As an example the vector $\vec{r}$ describes

the position of the global centre of gravity of the platform, tower and rotor. But it is also used to describe the position of panel corners or centres. The orientation of the platform is given with roll φ, pitch γ and yaw angle ψ with its linear time derivative $\vec{\omega} = \left[\dot{\varphi}, \dot{\gamma}, \dot{\psi}\right]^T$.

Panel method

Rotor and tower aerodynamics and the hydrodynamics of the platform are modelled in two different domains with different fluid parameters, but with synchronised motions. The base method of both domains is the same. Only some differences shall be mentioned later do describe the rotor wake in the aerodynamic or wave potential in the hydrodynamic domain.

Based on the assumption of an incompressible, irrotational and inviscid flow, the potential theory is capable to describe three-dimensional flow fields. Thereby, the velocity field is represented by a potential function Φ and the continuity equation can be reduced to the Laplace equation:

$$\Delta\Phi = 0 \, . \tag{1}$$

The velocity in the potential field is than given by its gradient

$$\nabla\Phi = \vec{v}_{pot} \, . \tag{2}$$

The total potential includes all potential flows in the simulation, in the following the wave and the induced potential:

$$\Phi = \Phi_{wave} + \Phi_{ind} \, . \tag{3}$$

The wave potential Φ_{wave} is defined below and only present in the hydrodynamic domain. The induced potential Φ_{ind} includes the influence of all panels in the domain.

To get the total flow velocity, the potential velocities are extended by the external flow velocity $\vec{v}_{ext}$. Hence, it results in a local body-fixed coordinate system with panel motion velocity $\vec{v}_{motion}$:

$$\vec{v} = \nabla \Phi_{ind} + \nabla \Phi_{wave} + \vec{v}_{ext} - \vec{v}_{motion} \tag{4}$$

The platform and the rotor are discretized using first-order panels with source and doublet strength. Based on the idea of a constant potential $\Phi = 0$ inside the closed body, a Dirichlet boundary condition is applied on each panel centre with a source strength σ equal to the normal velocity:

$$\sigma_i = (\nabla \Phi_{wave} + \vec{v}_{ext} - \vec{v}_{motion}) \cdot \vec{n}_i \tag{5}$$

$$-\frac{1}{4\pi}\int_i^n \sigma_i \frac{1}{r} dA_i + \frac{1}{4\pi}\int_i^n \mu_i \frac{\partial}{\partial \vec{n}_i}\left(\frac{1}{r}\right) dA_i = 0 \tag{6}$$

for n panels with the panel normal in outward direction $\vec{n}$, the distance between requested point and panel centre r and the area dA. Further information about the solving procedure and how to obtain a closed set of equation from equation (5) and (6) are given in (Katz 2001, page 237-249).

Bernoulli's equation for unsteady potential flow is then used to calculate the pressure on each panel.

$$\frac{p}{\rho} = \vec{g} \cdot \overrightarrow{r_p} - \frac{1}{2}(\nabla\Phi)^2 - \frac{\partial(\Phi)}{\partial t} \tag{7}$$

with the panel centre position $\overrightarrow{r_p}$, gravitational acceleration $\vec{g}$ and density ρ.

Additional frictional forces are added on each body panel based on the estimated local friction coefficient using the ITTC-1957 skin friction line.

Aerodynamics

When simulating lifting bodies, it is required to consider the circulation around the body. This is done by discretizing a wake surface which starts at the trailing edge of the blade. These wake panels deform freely with the flow and form a helix, its shape is influenced by the rotor speed and the flow velocity. In each time-step, new wake panels are inserted between the trailing edge and the fist wake panel. The circulation is induced by a non-zero doublet strength and is determined using the Kutta condition.

$$\mu_{wake\ panel} = \mu_{upper} - \mu_{lower} \tag{8}$$

Upper and lower subscript refer to the upper and lower body panel at the trailing edge. Once the doublet strength is set, it remains constant over time when the panel is transported downstream. Because the influence on the blade forces decreases with increasing distance and to limit the number of wake panels, the panel is removed when its age exceed a certain value. Further details and a stabilization method is described by Netzband et al. (2018).

In the aerodynamic domain, a symmetry condition is set at the undisturbed water line area. In addition, the wave potential in equation (3), (4) and (5) is omitted $\Phi_{wave} = 0$.

Hydrodynamics

The platform hull is discretized by source panels. Flow field and corresponding pressures are calculated based on the equations above. Additionally, an acceleration potential is calculated to improve the quality of the dynamic pressure and to allow for an advanced method of the added mass matrix calculation (see Netzband et al. 2018 and Sichermann 2008).

In the hydrodynamic domain, the seaway is a superposition of multiple regular

waves. The potential of a regular wave depends on position $\vec{r} = [x, y, z]^T$ and time t.

$$\Phi_{wave}(\vec{r}, t) = -\zeta_a \frac{2\pi}{kT} \frac{\cosh(k\,(z-d))}{\sinh(k\,d)} \mathrm{Re}\{i\, e^{i\,(-\omega t + k\,\bar{x} + \epsilon)}\} \qquad \text{(eq:wave)}$$

With the characterising values: wave amplitude ζ_a, angular wave frequency ω, wave number k and phase shift ϵ. The horizontal distance $\bar{x}$ is the distance of $\vec{r}$ in wave propagation direction. Panels which are above the wave surface are suppressed for the current point in time.

No special treatment is applied to handle the water surface as it is assumed that the floater is a transparent structure. Therefore radiation and diffraction effects are neglected. A verification study presented in the previous publication (Netzband et al. 2018) shows sufficient accuracy with this assumption.

Invisible force elements

Viscous effects on the platform and tower are not covered by the potential theory. Therefore additional surface elements are introduced. These elements evaluate the fluid velocity at their centre and calculate a resulting force based on direction dependent lift and drag coefficients. But they do not have any influence on the flow field. Originating from the idea of a blade element with a two-dimensional cross section they have a spanwise $\vec{a}_{v\perp}$ and chordwise direction $\vec{a}_{v\parallel}$. The local fluid velocity $\vec{v}$ is projected on the plane with a normal in spanwise direction $\vec{v}_l$. The resulting local velocity $\vec{v}_l$ has no component in spanwise direction and its angle to the chord direction α is used to estimate lift coefficient C_L and drag coefficient C_D. Using the a constant reference area A and the fluid density ρ, the three dimensional force results in equation (eq:Fils).

$$\vec{F}_{IF} = \underbrace{C_L(\alpha)\frac{\rho}{2}A(\vec{v}_l \times \vec{a}_{v\perp})|\vec{v}_l|}_{Lift} + \underbrace{C_D(\alpha)\frac{\rho}{2}A \cdot \vec{v}_l|\vec{v}_l|}_{Drag} \qquad \text{(eq:Fils)}$$

These force elements are used in two ways; for the tower and the hull drag of the platform.

Dynamic mooring

The implemented mooring line model is based on the formulation given by Hall and Goupee (2015). It is based on a lumped mass approach with connecting spring damper elements and covers inertia effects as well as forces by induced, current, motion velocities and accelerations. Wave forces are neglected. Because of its relatively large stiffness at least in line direction, comparatively small time-steps are necessary compared to the global time-step of the simulation. Therefore a global time-step is divided into small mooring time-steps. Within one global time-step deformation and velocities of the fairlead nodes are interpolated using a non-linear approach to achieve smooth transitions of the fairlead motions across the global time-steps. A fourth order Runge-Kutta method is applied to integrate the motions during the internal mooring time steps. The implementation is also able to follow the higher order time integration scheme of the global motions, see below.

6DOF and time marching

Predicting the motions of the platform is immanent, when analysing the self-aligning capability of the platform. Furthermore, the current position and motion state of platform, turbine and mooring have major influence on the forces. In this simulation, a six-degrees-of-freedom (6DOF) solver has been applied to estimate the motions. The entire structure (platform, tower, rotor blades) is assumed to be rigid, only the rotor has an additional degree of freedom to rotate freely. By solving the Newton-Euler equations the acceleration of the platform is calculated in general coordinates in the global coordinate system (see Figure fig:COS).

As already mentioned in the previous paper (Netzband et al. 2018), a fourth-order Runge-Kutta method is applied to integrate the motion of the platform in six-degrees-of-freedom (6DOF). Motions of rotor, tower and mooring fairlead are synchronized with the platform. No changes have been done on this parts of the method.

Structural design

The basic idea of this FWOT concept, is the windvaning capability of the entire platform by taking advantage of the wind aligning moments of a downwind turbine with large cone angle and profiled tower combined with a pivotable single point mooring. The semi-submersible design of the platform consists of four columns and a diamond bottom structure with a length of 80 m and a width of 55 m. When ballasted, the total draft is 13 m and the freeboard is 10 m. The tower is placed on one column and is supported by two diagonal (struts) legs sitting on the lateral columns. They all have a NACA0035 profile facing the leading edge in upwind direction. A chord length of 8 to 12 m on the tower and 6m on the legs ensure a large restoring moment when not aligned in the wind direction, see Figure fig:selfaligning (a). When aligned with the wind, the symmetrical profile reduces the tower shadow and its impact on the blades of the downwind turbine placed on top of the tower, see Figure fig:selfaligning (b). No yaw bearing is required at the top, the nacelle has a fixed connection. The SCD 6MW turbine is pitch regulated turbine and can have two or three blades. Only the two bladed configuration is used in the current work mainly because it's lower weight. Characterising parameters of the rotor are given in table tb:rotor. The single point mooring is attached on the fourth column. It is equipped with a turret system to pivot freely around its centre point. Detailed information are given in table tb:mooring. The power cable passes through the middle of the mooring and a slip ring avoids twisting.

The entire platform has a little trim angle of $0.9°$ when turned off. With the maximum thrust at rated conditions, the platform pitches backword to a mean value of $-2°$. No active ballast water system is installed. The global properties of the platform, tower and rotor are given in table tb:global.

Table tb:rotor: Specifications of the SCD 6MW downwind turbine of aerodyn	
Rated Power (electrical)	6 MW
Number of blades	2
Diameter	140 m
Hub height above still water line (SWL)	90 m
Nominal rotor speed	13.6 1/min
Nominal wind speed	12.1 m/s

Table tb:mooring: Specifications of the mooring system	
Number of lines	5
Unstretched line length	350 m
Line diameter	0.089 m
Mass per unit length in water	175 kg/m
Axial rigidity / extensional stiffness (EA)	735 MN
Anchor radius	344 m
Water depth	40 m
Total static vertical pull	720 kN

Table tb:global: Global properties (including rotor, tower and ballast)

Mass	7880 t
COG below SWL	2.4 m
Inertia Matrix	$\begin{bmatrix} 5.94 & 0 & 1.72 \\ 0 & 8.30 & 0 \\ 1.72 & 0 & 6.19 \end{bmatrix} \times 10^6 \text{ t m}^2$

Simulation Setup

A global overview on the simulation setup is given in Figure fig:model with all discretised parts, the rotor wake and the mooring lines. The water surface is also indicated.

On the turbine, nacelle and hub are neglected. The cylindrical part of the rotor blades has also been omitted, because inaccuracies can be induced by stall regions near the blade root. The air foil shaped part of the blade has been modelled using 2520 body panels with a refinement on root and tip as well as on the leading and trailing edge, see Figure fig:griddetails (a). In accordance to the lengths of the trailing edges, the wake shape is refined on tip and hub to improve the rollup of the wake. In total 8000 wake panels are used to model the wake in a length of at least two rotor diameters. To capture ground effects which can occur at the water surface, a symmetry condition is applied with at the SWL. A 1DOF solver with a rotor speed to generator torque table allows free rotation of the rotor. But no pitch controller is implemented. Hence the wind speed of the simulation is limited to values below the rated wind speed of the turbine.

Due to the relatively thick NACA0035 profile of the tower, a modelling with lifting panels has given large discrepancies regarding the lift forces. Therefore the tower is represented by 30 invisible lifting elements. These elements are described above and the reference area is visible in Figure fig:model and fig:griddetails (a). They do not influence the flow field and hereby do not interact between with the rotor and its wake.

However, the tower shadow effect only has relatively small influence on the global platform alignment. The more important influence from the rotor on the tower by its induced velocity is captured as the global fluid velocity is used to estimate the lift and drag forces of the tower. The lift and drag coefficients of the NACA0035 profile were used according to the experimental results presented in Sarraf et al (2010).

The platform is discretised with 4492 body panels. A refinement is applied in the region of the water surface to increase the resolution of the wetted hull surface, see Figure fig:griddetails (b). A grid study has been conducted and Figure fig:gridstudy shows the result of the calculated added mass in surge, sway and heave direction for three numbers of panels. A convergence is clearly visible and the selected resolution has an error below 2.5 %.

Because of the lack of viscous effects in potential flow, 60 additional invisible force elements are used include hull drag effects of the platform, see Figure fig:griddetails (c). These elements only consider the external flow and wave velocity and the bodies' motion velocity. The induced velocity is ignored referring to the definition of lift and drag coefficients to be dependent on the undisturbed fluid velocity. In length (or span) direction, the platform components are divided into multiple elements. The chord direction defines the orientation of the elements. In table tb:platformcoeff the drag coefficients related to the angle between chord direction and fluid velocity are given

In total 150 mooring elements are used. The nodes are equally distributed over the line and have the same local fairlead position in the centre on the bottom of the fore column. Seaway is represented by a superposition of regular waves. In the presented load cases, JONSWAP spectra with uniform wave direction are used. The density of air is set to $1.24\ \mathrm{kg/m^3}$ with a viscosity of $1.48 \times 10^{-5}\ \mathrm{m^2/s}$, while the density of water

set to $1025\ \mathrm{kg/m^3}$ with viscosity of $1.0 \times 10^{-6}\ \mathrm{m^2/s}$. A global time-step of 0.1 s is used. The internal mooring time step is set to a much lower value of 0.005 s.

Table tb:platformcoeff: Drag coefficients for platform hull drag

Part	**Relative Flow direction**	
	0°	**90°**
Rectangular (diamond)	0.75	1.5
Hexagonal (front and rear column)	1.2	1.2
Hexagonal (lateral column)	0.8	1.2

Simulations

Two sets of simulations have been conducted to analyse the self-aligning capability of the platform. First, the power production and misalignment is shown for a partial turbine load and for different wind-current misalignments. In a second section, the unsteady behaviour is shown for a change of wind speed and direction.

Steady alignment

A central question in the design is the ability of the platform to align with the wind under oblique current and/or waves. To estimate the resulting yaw error of the turbine and to analyse the restoring moment, the power curve is simulated with various wind-current misalignments. The simulation is limited to partial load where the blade pitch is constant. In table tb:steadycond the simulated wind speed and corresponding current, wave height and peak period of the uniform JONSWAP spectrum are given. The current is composed of a constant sea current of $0.5\ \mathrm{m/s}$ and a surface flow depending on the

wind speed. Each wind speed is simulated with a wind-current misalignment of 0, 30 and 60 degree. The wave propagation direction is the same as the current one.

In Figure fig:motions the wave elevation and platform heave, roll, pitch and yaw motion are shown for a wind speed of 10.5 m/s with wind and current aligned. The heave motions are dominated by the eigenfrequency of the platform, which has a value of 12.4 s. Both, roll and platform pitch have a little offset, coming from the turbine moment and thrust. An offset is also clearly visible in the platform yaw motion. This offset is mainly induced by the small heel angle, which moves the centre of thrust of the turbine some distance in sideways direction and result in a yaw moment around the turret system. A reduction could be achieved by relocating around 11 t ballast water from one lateral column to the opposite column to add a counteracting heel moment. The global position of the centre of mass has been moved only 0.066 m to the side. But in the result the heel angle was reduced below 0.1° for a wind speed of 10.5 m/s. Of course, for lower rotor torques under partial conditions a heel angle occurs, though above nominal conditions the generator torque is constant and therefore compensated.

The platform yaw angle and corresponding yaw moments from platform, tower and rotor are shown in Figure fig:turretmoment for all misalignment angles. All are mean values over a length of 100 s after the platform motions converged. Heeling the platform reduced the yaw misalignment for a current with zero degree. With current angles of 30° yaw misalignments above 10° occur but they stay below 20° even for lower wind speeds when the rotor thrust is reduced and less lift forces act on the tower. Larger misalignment occur when the current has an angle of 60°. The yaw moments around the turret system are shown in the upper part of the figure. With increasing wind speed, the aerodynamic forces become larger and reduce yaw misalignments. Similarly,

the yaw moment of the platform, mainly the coming from the drag, increases. For all conditions the restoring moment is dominated by the tower.

The influence on rotor thrust and power is shown in Figure fig:turbinedata. All values are normalized with the maximum thrust respectively power. The yaw misalignment under current angles lead to a reduction of thrust and torque. For 30° the thrust is only 1.7% and the power 3.0% lower at 11.8 m/s. But at 60° a power loss of 12% occurs. The lower aerodynamic yaw moment at lower wind speeds increases the relative loss. At a wind speed of 5.2 m/s a misalignment of 30° lead to 10% and 60° even to 45% of power loss. However, these wind speeds do not contribute very much to the total energy production over a year.

No simulations have been done for wind speeds above nominal conditions. But a good self-aligning behaviour can be assumed from the tendency of Figure fig:turretmoment. In stronger winds, the blades will be pitched out to get a constant power. This reduces the rotor thrust and its part on the self-aligning moment. But more important, the lift forces on the tower will increase because of the higher incident flow.

Table tb:steadycond: Environmental conditions for load curve

Wind speed	**Sign. wave height**	**Peak period**	**Current**
[m/s]	**[m]**	**[s]**	**[m/s]**
5.2	1.2	6.72	0.57
7.9	1.88	7.41	0.61
10.5	2.85	8.38	0.64
11.8	3.44	8.96	0.66

Unsteady alignment

When wind speed and direction changes, the platform starts to move and finds a new position. In a second set of simulations, the presented method is used to simulate a dynamic, non-period motion. Based on the formulas for a gust by DNV GL (2012), section 4.2.2.4, an increasing wind velocity and change of direction is simulated. With the initial wind velocity $v_0 = 8\ \mathrm{m/s}$, a delta of $v_{cg} = 3\ \mathrm{m/s}$ and changing lengths T of 90 s, 180 s and 360 s, the wind velocity $v_{ext,air}$ is given by

$$v_{ext,air}(t) = \begin{cases} v_0 & \text{for } t < t_g \\ v_0 + 0.5 v_{cg}(1 - \cos(\pi t/T)) & \text{for } t_g \leq t \leq t_g + T \\ v_0 + v_{cg} & \text{for } t > t_g + T \end{cases}$$

The direction changes of $\Omega_{cg} = 0°$, 30° and 60° define the wind direction Ω accordingly.

$$\Omega(t) = \begin{cases} 0 & \text{for } t < t_g \\ 0.5\Omega_{cg}(1 - \cos(\pi t/T)) & \text{for } t_g \leq t \leq t_g + T \\ \Omega_{\mathrm{cg}} & \text{for } t > t_g + T \end{cases}$$

The start of the changing wind is set to $t_g = 200$ s for all scenarios to ensure steady platform motions at the beginning. An exemplary wind velocity is shown in Figure fig:gustwindvel for a length $T = 90$ s. The grey area marks the time during the change and is used some following likewise.

When the wind speed increases, the average rotor thrust increases and lead to a platform pitch motion. Without wind direction change, this is shown in Figure fig:gustptich. The grey line marks the beginning of the change with lengths of 90 s, 180 s and 180 s. While a length of 90 s leads to an overshoot, on longer times of change the platform pitch is smooth.

The influence of a wind direction change on the turbine power during a change of the wind speed is shown in Figure fig:gust90 to fig:gust360. A short length of 90 s, shown in Figure fig:gust90, leads to a maximum yaw misalignment of 20° for a direction change of 30° and corresponding power loss. After 40 s the yaw misalignment is reduced below 10° and negligible loss. A direction change of 60° lead to much higher misalignment of 47°. The rotational speed of the rotor collapses and thus also the thrust and power. It is the lift forces of the tower which makes a major contribution to the yaw moment in this situation and pushes the self-aligning. As a result, the yaw misalignment is above 10° for a total length of 137 s. Doubling the time of the change, shown in Figure fig:gust180, leads to a lengthening of the effect. For a direction change of 60° the maximum misalignment angle of 30° is lower, but the stays over 10° for 155 s. At a length of 360 s for the change in wind velocity, the misalignment is above 10° for 173 s, see Figure fig:gust360. Anyway, the loss of energy is lower, with increasing time for the change of wind velocity, as the rotor operation does not collapse due to moderate maximum misalignment angles on longer times.

Conclusion

The dynamic transverse and longitudinal stability as well as the yaw behaviour of the SelfAligner, a self-aligning FOWT, are analysed with the first-order panel method *pan*MARE. The simulations of the motion behaviour of the FOWT are carried out for various environmental conditions with regard to wind, natural waves and current. The mooring Forces are calculated using a dynamic mooring model. Due to the lack of a pitch controller for the blades of the wind turbine, the wind speed is limited to partial load conditions. The results of the investigation show that a strong coupling between aerodynamics and hydrodynamic loads as well as mooring system induced

forces in the simulations is essential for the evaluation of the self-aligning behaviour of the FOWT.

The resultant rotor moment shows a small eccentricity, which induces a heel and yaw moments. A small heel angle can have a considerable influence on the alignment due to the high rotor forces. Therefore it will be an advantageous to reduce the heel angle by using asymmetric ballast water distribution to balance the transvers aerodynamic moment induced by the rotor.

The influence of relatively strong currents from 0.57 m/s to 0.66 m/s depending on the wind speed on the self-aligning capability is investigated. Moderate misalignment angles are predicted for 30° of wind-current misalignment. On 60° high yaw errors above 20° occur. As it is expected, the misalignment increases at lower wind speeds due to low aerodynamic forces. A closer look at the contributions of the different components of FOWT to the aligning moment shows that the main component is delivered by of the profiled tower. Especially at higher wind speeds, the tower influence becomes more important and contribute significantly to align the platform.

In the concept studied, the reaction time of the floating structure to the misalignment of the between wind and turbine at low wind speeds represents a major challenge. Therefore, these inappropriate operating conditions were investigated. Under dynamic wind direction change, the platform reacts slowly but is capable to follow a wind direction change of 30° within 180 s. Larger angles or faster changes lead to temporary misalignment, and the FOWT will require more time to generate the corresponding alignment moment. Even a momentarily break-in of the rotational speed can occur when the wind turns suddenly with a large angle, but the generated yaw moment of the tower will quite effectively be able to reduce the misalignment of the

FOWT. The required time is comparable with conventional turbine designs including a yaw bearing because of controller delay low yaw speeds.

Acknowledgements

The authors kindly thank our project partners Cruse Offshore GmbH, aerodyn engineering gmbh, JÖRSS – BLUNCK – ORDEMANN GmbH, DNV-GL and the Institute for Ship Structural Design and Analysis at the Hamburg University of Technology for the excellent cooperation.

Disclosure statement

No potential conflict of interest was reported by the authors.

Funding

The authors kindly thank the Federal Ministry for Economic Affairs and Energy of Germany (BMWi) for financially supporting the HySToH project [03SX409A-F].

References

DNV GL. 2012. Guideline for the Certification of Offshore Wind Turbines. Hamburg.

Hall M, Buckham B, Crawford C. 2014. Evaluating the importance of mooring line model fidelity in floating offshore wind turbine simulations. Wind Energy. 17:657–669.

Bauer M, Abdel-Maksoud M. 2012. A 3-D Potential Based Boundary Element Method for Modelling and Simulation of Marine Propeller Flows. In: 7th Vienna Int. Conf. Math Model. Vol. 7. Vienna; p. 1179–1184.

Cordle A, Jonkman J. 2011. State of the Art in Floating Wind Turbine Design Tools. Renew. Energy 8:367–374.

Hall M, Goupee A. 2015. Validation of a lumped-mass mooring line model with DeepCwind semisubmersible model test data. Ocean Eng. 104:590–603.

Hundemer J. 2013. Entwicklung eines Verfahrens zur Berechnung der instationären potenzialtheoretischen Propellerumströmung [dissertation]. Hamburg: Hamburg University of Technology.

Katz J, Plotkin A. 2001. Low-Speed Aerodynamics. Cambridge (UK): Cambridge UP. (Aerospace Series).

Laino DJ, Hansen AC, Minnema JE. 2002. Validation of the AeroDyn subroutines using NREL unsteady aerodynamics experiment data. Wind Energy 5:227–244.

Masciola M. 2015. MAP ++ Documentation.

Netzband S, Schulz CW, Göttsche U, Ferreira Gonzales D, Abdel-Maksoud M. 2018. A Panel Method for Floating Offshore Wind Turbine Simulations with Fully-Integrated Aero- and Hydrodynamic Modelling in Time Domain. Sh Technol Res. 0:1–14.

Sarraf C, Djeridi H, Prothin S, Billard JY. 2010. Thickness effect of NACA foils on hydrodynamic global parameters, boundary layer states and stall establishment. J Fluids Struct. 26:559–578.

Schoop-Zipfel J, Abdel-Maksoud M. 2014. Maneuvering in Waves Based on Potential Theory. In: 33rd Int. Conf .Ocean Offshore Arct Eng. Vol. 8B. San Francisco (CA).

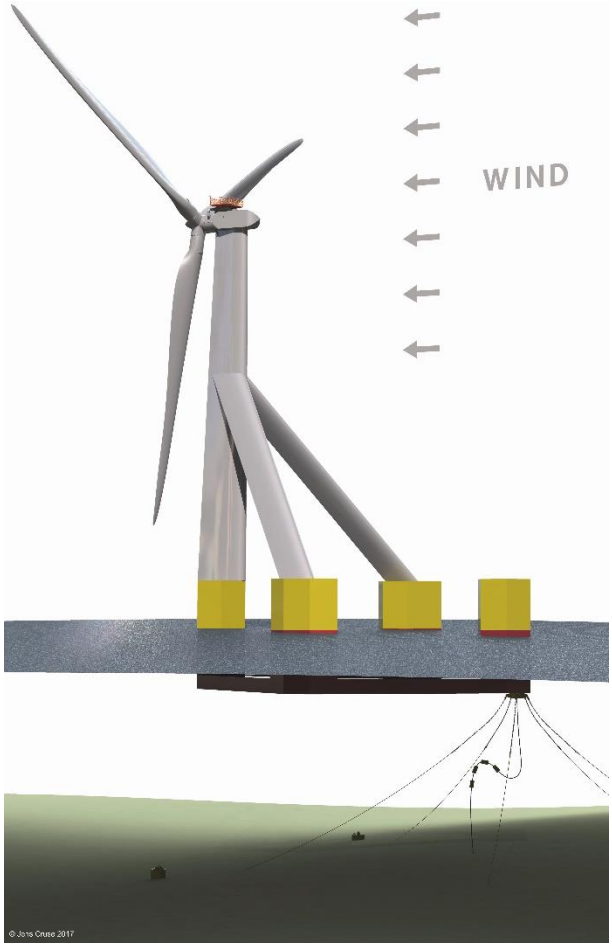

Figure fig:LOFT. The SelfAligner designed by Cruse Offshore GmbH

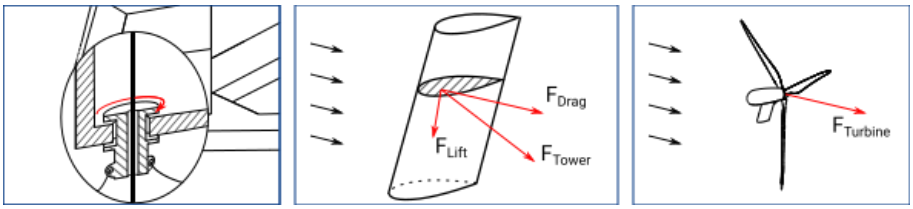

(a) Single point mooring and self-aligning forces

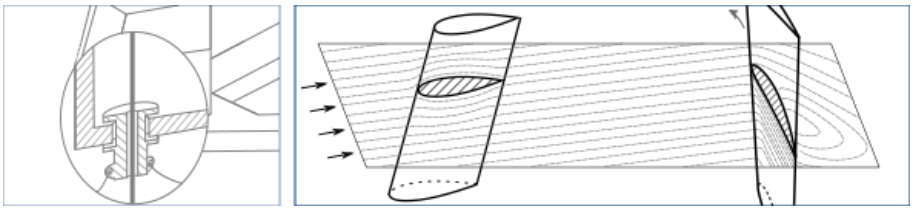

(b) Reduced tower shaddow effects on the downwind rotor

Figure fig:selfaligning. Single point mooring, profiled tower and downwind rotor

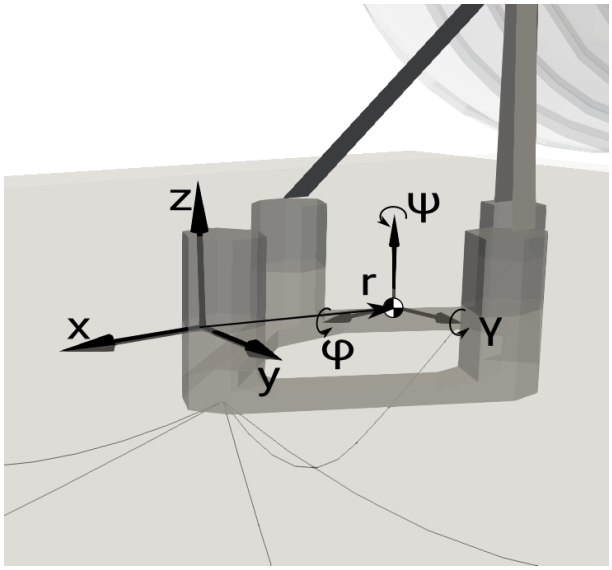

Figure fig:COS. General coordinate system

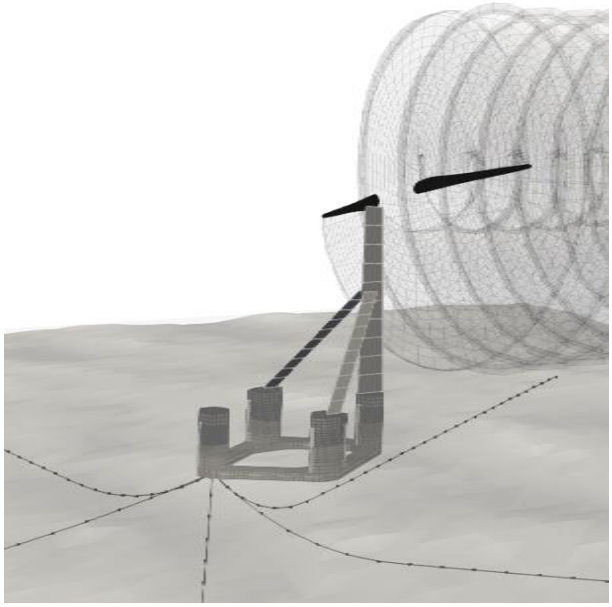

Figure fig:model. Model setup with platform, tower, rotor blades, rotor wake and mooring

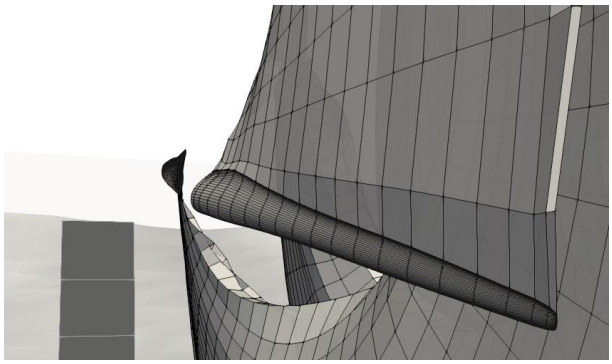

(a) Rotor and wake grid

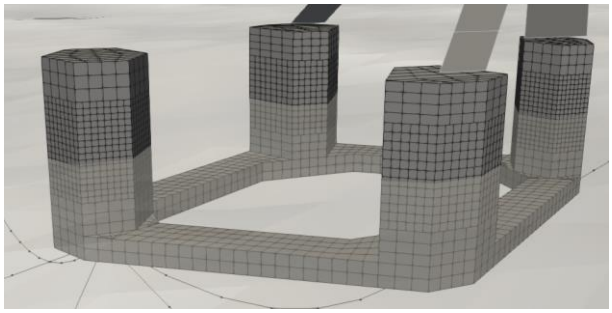

(b) Platform grid

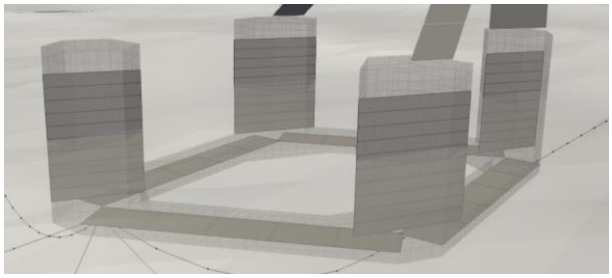

(c) Platform drag elements

Figure fig:griddetails. Grid details

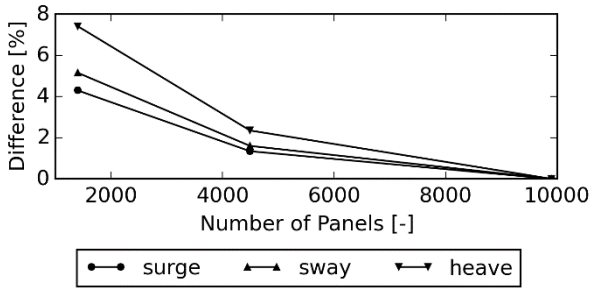

Figure fig:gridstudy. Relative difference of the hydrodynamic mass in surge, sway and heave direction for different amount of panels.

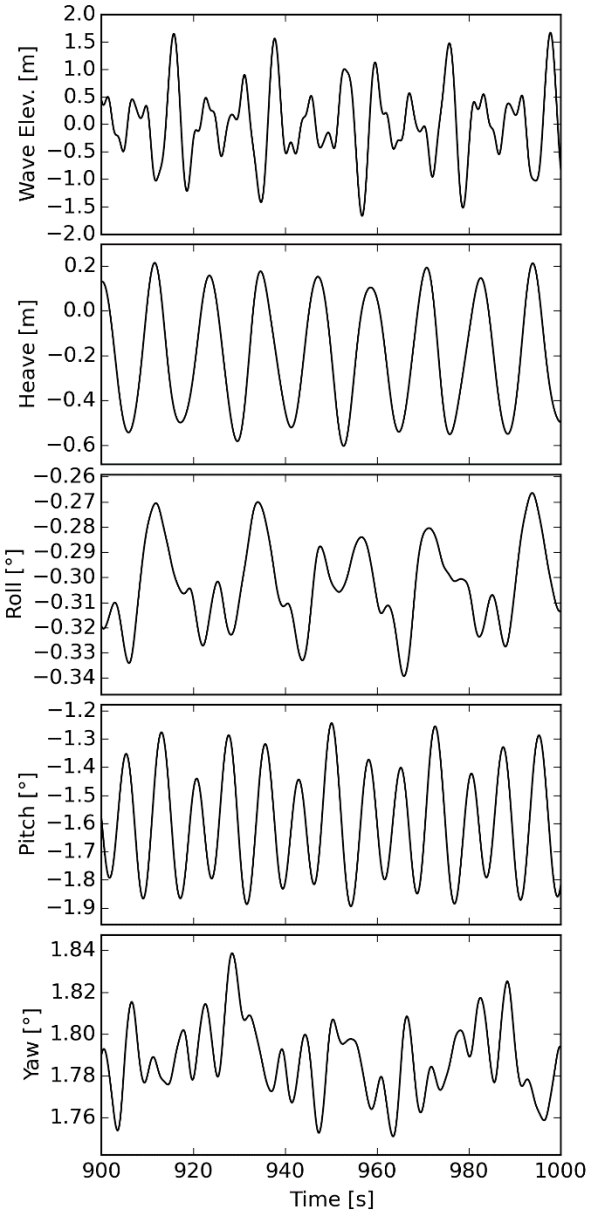

Figure fig:motions: Wave elevation and platform motions over time for 10.5 m/s wind and no misalignment.

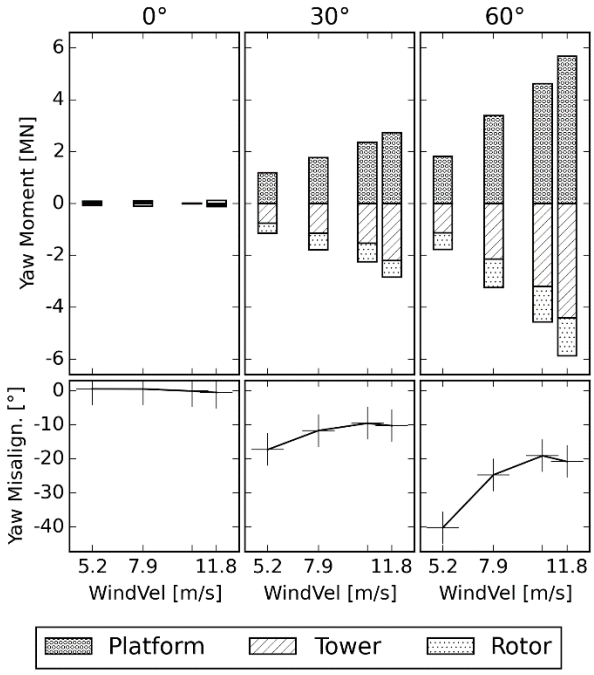

Figure fig:turretmoment. Turret moments and platform misalignment for different current-wind angles and wind velocities. A negative moment aligns with the wind direction.

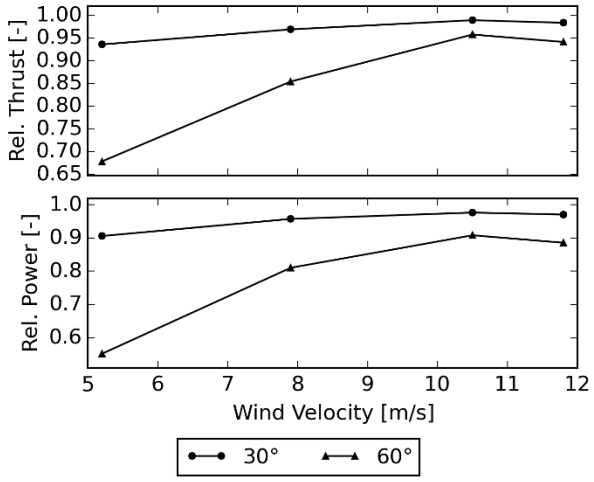

Figure fig:turbinedata. Turbine data of the heeled platform over wind speed for different wind-current misalignments related to uniform wind-current.

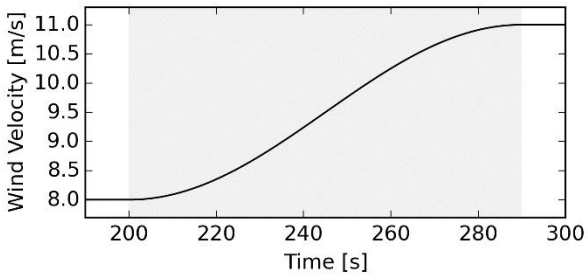

Figure fig:gustwindvel. Wind velocity for a change of wind velocity with length of 90 s.

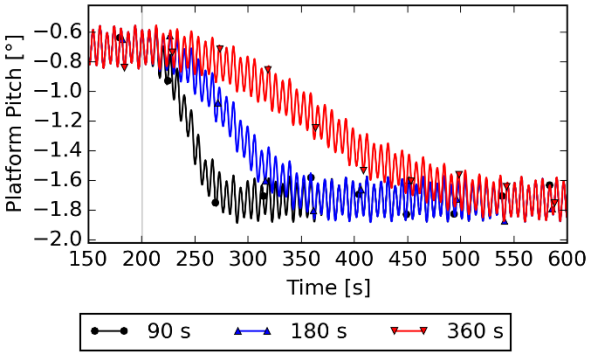

Figure fig:gustptich. Platform pitch motion for changing winds of different lengths but no wind direction change.

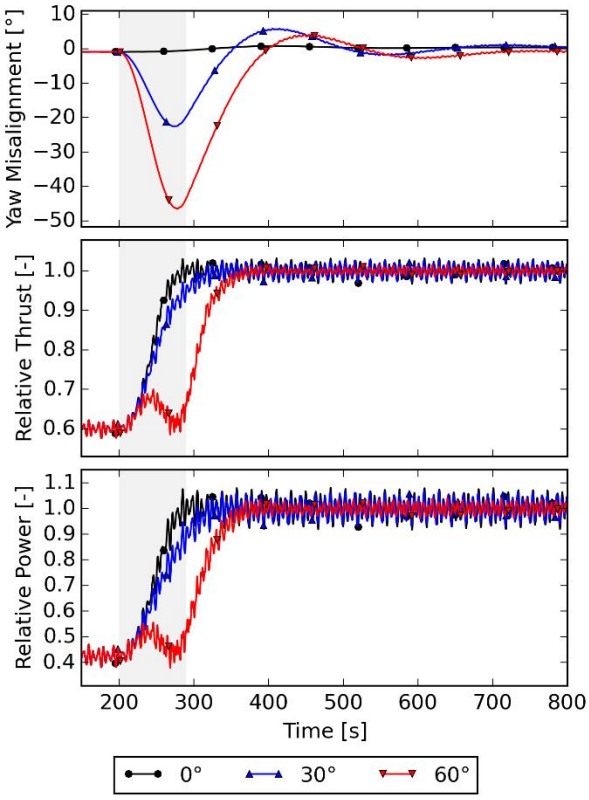

Figure fig:gust90. Turbine data for a wind change with length of 90 s. Thrust and power is related to values at wind of 11 m/s.

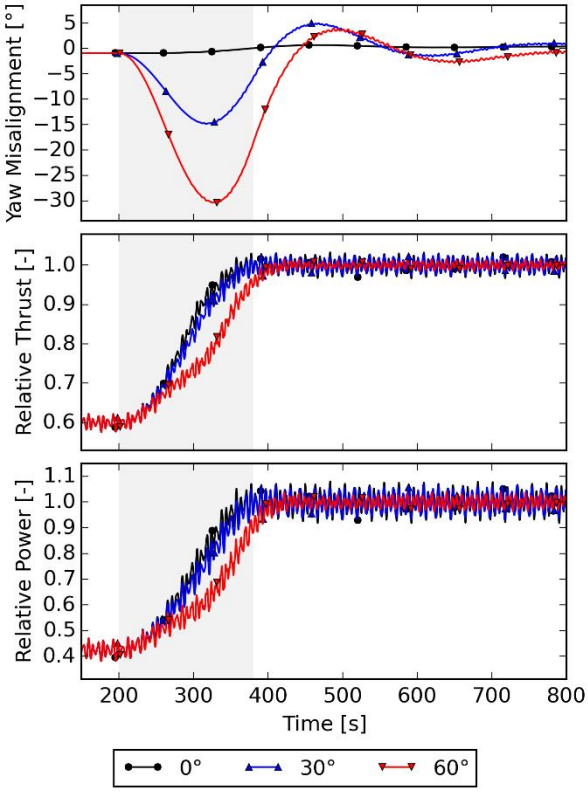

Figure fig:gust180. Turbine data for a wind change with length of 180 s. Thrust and power is related to values at wind of 11 m/s.

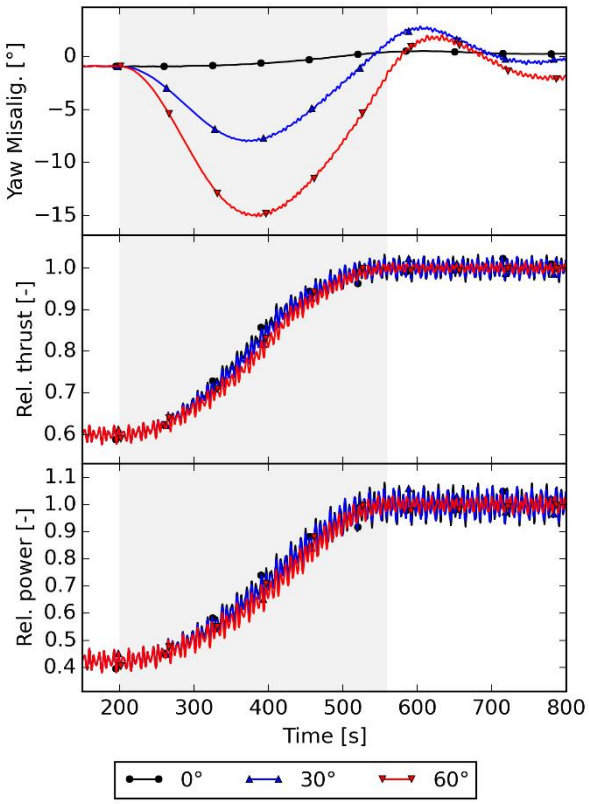

Figure fig:gust360. Turbine data for a wind change with length of 360 s. Thrust and power is related to values at wind of 11 m/s.